Reducing Uncertainty in Damage Growth Properties by Structural Health Monitoring

Alexandra Coppe[1], Raphael T. Haftka[1], Nam-Ho Kim[1] and Fuh-Gwo Yuan[2]

[1] *University of Florida, Gainesville, FL, 32611, USA*
alex.coppe@academic.edu
haftka@academic.edu
nkim@ufl.edu

[2] *North Caroline State University, Raleigh, NC, 27695, USA*
yuan@ncsu.edu

ABSTRACT

Structural health monitoring provides sensor data that monitor fatigue-induced damage growth in service. This information may in turn be used to improve the characterization of the material properties that govern damage propagation for the structure being monitored. These properties are often widely distributed between nominally identical structures because of differences in manufacturing processes and aging effects. The improved accuracy in damage growth characteristics allows more accurate prediction of the remaining useful life (RUL) of the structural component. In this paper, a probabilistic approach using Bayesian statistics is employed to progressively reduce the uncertainty in structure-specific damage growth parameters in spite of noise and bias in sensor measurements. Starting from an initial, wide distribution of damage parameters that are obtained from coupon tests, the distribution is progressively narrowed using the damage growth between consecutive measurements. Detailed discussions on how to construct the likelihood function under given noise of sensor data and how to update the distribution are presented. The approach is applied to crack growth in fuselage panels due to cycles of pressurization and depressurization. It is shown that the proposed method rapidly converges to the accurate damage parameters when the initial damage size is 20mm and there is no bias in the measurements. Fairly accurate material properties can be obtained also with measurement errors of 5mm. Using the identified damage parameters, it is shown that the 95% conservative RUL converges to the true RUL from the conservative side. The proposed approach may have the potential of turning aircraft into flying fatigue laboratories.*

1 INTRODUCTION

Structural health monitoring (SHM) will have a significant impact on increasing safety as well as reducing the operating and maintenance costs of structures by providing an accurate quantification of degradation and damage at an early stage to reduce or eliminate malfunctions. Furthermore, SHM will allow predictions of the structure's health status and remaining useful life (RUL) without intrusive and time consuming inspections. Continual on-line SHM is based on dynamic processes through the diagnosis of early damage detection, then prognosis of health status and remaining life.

Prognosis techniques can be categorized based on the usage of information: (1) physics-based, (2) data-driven, and (3) hybrid methods. The physics-based method, or model-based method in Luo, et al. (2003), assumes that the system behavior is known. Dynamic stochastic equation, lumped-parameter model in Li and Lee (2005), and functional models in Berruet, et al. (1999) correspond to this category. In the case of SHM, crack growth model in Li and Lee (2005), Ray and Patankar (1999, Ray and Tangirala (1996) or spall growth models are often used for micro-levels, and first principle models in Jaw, et al. (1999) are used for macro-levels.

The data-driven method in Schwabacher (2005) uses information from collected data to predict future status of the system, and includes least-square regression in Montanari (1995) and Xue, et al. (2007), Gaussian process regression in Goebel, et al. (2008) and Srivastava and Das (2009), neural network in Jaw, et al. (1999), Goebel, et al. (2008) and Srivastava and Das (2009), and relevance vector machine in Goebel, et al. (2008) and Tipping (2000). This method has advantages when the system is so complex that no simple physical model is available. The hybrid method in Yan and Lee (2007) uses the advantages from both methods, and includes particle filters in Orchard, et al. (2008) and Bayesian techniques in Sheppard, et al. (2005) and Saha and Goebel (2008). It is generally accepted that uncertainty is the most challenging part for prognosis in Saha and Goebel (2008) and Engel, et al. (2000). Sources of uncertainty are initial state estimation, current state estimation, failure threshold, measurement, future load, future environment, and models. In order to address the uncertainty, various methods have been proposed, such as confidence intervals in Gu, et al. (2007), relevance vector machine in Goebel, et al. (2008), Gaussian process regression in Goebel, et al. (2008) and Srivastava and Das (2009), and particle filers in Orchard, et al. (2008) and Orchard, et al. (2005).

The current technology of diagnosis and prognosis using sensor-based SHM anticipates difficulties associated with uncertainties in sensor data, damage growth models, and material and geometric properties. The first is related to identifying the current health status, while the others are related to predicting the health status in the future. Uncertainties in sensor data can be classified in two categories: the systematic departure due to bias and the random variability due to noise. The former is caused by calibration error, sensor location and device error, while the latter is caused by measurement environment. Note that bias may tend to vary non-randomly as the crack grows due to the nature of the error, for example the placement of the sensor being focused on the growth direction of the crack, the bias may decrease as the crack grows. However, we assume the bias to be constant over the entire life of the structure.

Compared to manual inspections, the accuracy of SHM is still poor. The minimum detectable size of damage using SHM is much larger than that of manual inspection methods. In addition, the measured data have the aforementioned noise and bias. Thus, the major challenge is how to accurately predict the damage growth when the measured data include both noise and bias. However, unlike manual inspection, SHM may provide frequent measurements of damage, allowing us to track damage growth. This in turn, should allow us to reduce the uncertainty in the material properties that govern damage growth. The uncertainty in these properties is normally large because of noise in manufacturing and aging of the monitored structured. The main objective of this paper is to demonstrate the reduction in uncertainty that may be achieved using abundance in data. A probabilistic approach using Bayesian statistics is employed to progressively improve the accuracy of predicting damage parameters under noise and bias of sensor measurements.

The proposed approach is demonstrated using a through-thickness crack in an aircraft fuselage panel which grows through cycles of pressurization and de-pressurization. A simple damage growth model, Paris model by Paris, et al. (1999), with two damage parameters is utilized. However, more advanced damage growth models can also be used, which usually comes with more parameters. Using this simple model we aim to demonstrate that SHM can be used to identify the damage parameters of each particular panel. This process can be viewed as turning every aircraft into a flying fatigue laboratory. Reducing uncertainty in damage growth parameters can reduce in turn the uncertainty in predicting remaining useful life (RUL), i.e. in prognosis. Improved knowledge on RUL can have practical consequences such as increased time between visual inspections based on the conservative estimation using actual data, or a reduction in hardware testing when SHM is combined with manual inspection.

The paper is organized as follows. In Section 2, a simple damage growth model based on Paris model is presented. The current paper is based on data obtained from a previous work from Kale et al. (2003, 2004 and 2008), which describes the fatigue crack growth in a fuselage panel of 7075-T651 aluminum alloy. In section 3 the measurement model is introduces, it shows how error in measurements due to SHM is added to the model presented in the previous section it also presents how Bayesian updating is used to identify the damage parameters. In section 4 the numerical application of the model is presented. In Section 5, the updating of damage parameter m is presented as well as the prognosis results resulting from it. In Section 6, results similar at the one presented in section 5 but obtained updating the other damage parameter, C. Conclusions are presented in Section 7 along with future plans.

2 DAMAGE GROWTH MODEL

The Damage in a structure starts from the microstructure level, such as dislocations, and they gradually grow to the level of detectable macro-cracks through nucleation and growth. Damage in the micro-structure level grows slowly, is difficult to detect, and

is not dangerous for structural safety. Thus, SHM often focuses on macro-cracks, which grow relatively quickly due to fatigue loadings.

Once the damage reaches a detectable size, various SHM techniques can be employed to evaluate the current state of structural health by measuring the size of damage (Wang and Yuan (2005)). In the physics-based prognosis techniques, it is necessary to incorporate the measured data into a damage growth model to predict the future behavior of the damage. Since the damage growth model is not the main focus of the paper, the simplest model by Paris, et al. (1999) is used in this paper. However, more advanced models can also be applied using the same concept.

In this paper, we consider a fatigue crack growth in a fuselage panel with initial crack size a_i subjected to fatigue loads with constant amplitude due to pressurization. The hoop stress varies between a maximum value of σ to a minimum value of zero in one flight. One cycle of fatigue loading represents one flight. Like many other researchers (e.g., Harkness (1994) and Lin, et al. (2002)), we use the damage growth model by Paris, et al. (1999) as

$$\frac{da}{dN} = C(\Delta K)^m \tag{1}$$

where a is the crack size in *meters*, N the number of cycles (flights), da/dN the crack growth rate in *meters/cycle*, and ΔK the range of stress intensity factor in $MPa\sqrt{meters}$. The above model has two damage parameters, C and m. Accurate prediction of these parameters is important in predicting the remaining useful life of a particular panel.

The range ΔK of stress intensity factor for a center-cracked panel is calculated as a function of the stress σ and the crack length a in Eq. (2), and the hoop stress due to the pressure differential p is given by Eq. (3)

$$\Delta K = \sigma\sqrt{\pi\frac{a}{2}} \tag{2}$$

$$\sigma = \frac{pr}{t} \tag{3}$$

where p is the magnitude of pressure, r is the fuselage radius, and t is the panel thickness. Equation (2) does not include a geometric correction factor due to finite size of the panel, and Eq. (3) does not include corrections due to the complexity of the fuselage construction, so that they are both approximate.

The number of cycles N of fatigue loading that makes a crack to grow from the initial crack size a_i to the final crack a_N can be obtained by integrating Eq. (1) between the initial crack a_i and the final crack a_N.

$$N = \int_{a_0}^{a_N} \frac{da}{C\left(\sigma\sqrt{\pi a}\right)^m} = \frac{a_N^{1-\frac{m}{2}} - a_0^{1-\frac{m}{2}}}{C\left(1-\frac{m}{2}\right)\left(\sigma\sqrt{\pi/2}\right)} \tag{4}$$

Alternatively, the crack size a_N after N cycles of fatigue loading can be obtained by solving Eq. (4) for a_N.

$$a_N = \left(NC\left(1-\frac{m}{2}\right)\left(\sigma\sqrt{\frac{\pi}{2}}\right)^m + a_0^{1-\frac{m}{2}}\right)^{\frac{2}{2-m}} \tag{5}$$

The panel will fail when the crack reaches a critical crack size, a_C. Here we assume that this critical crack size is when the stress intensity factor exceeds the fracture toughness K_{IC}. This leads to the following expression for the critical crack size (again neglecting finite panel effects)

$$a_C = \left(\frac{K_{IC}}{\sigma\sqrt{\pi/2}}\right)^2 \tag{6}$$

3 STATISTICAL CHARACTERIZATION OF DAMAGE PROPERTIES USING BAYESIAN UPDATING

As mentioned in the previous section, the damage parameters, C and m, are critical factors to determine the growth of damage. These parameters are normally measured using fatigue tests under controlled laboratory tests. However, uncertainty in these parameters is normally large because of variability in manufacturing and aging of the specific panel. It is possible to curve fit the data and obtain estimates of these parameters for the individual panel. However, curve fits do not take into account prior information on the distribution of these parameters, nor statistical information on the measurement uncertainty. We therefore use Bayesian statistics to identify these parameters.

As can be found in Fig. 1, the parameter C corresponds to y-intercept at m = 1, of the fatigue curve, while the exponent m is the slope of the curve in the log-log scale. Kale (2003, 2004 and 2008) showed that the effect of exponent m is more significant than that of C on damage growth. As a first step in developing a prognosis methodology, we assumed that the accurate value of C is known, while that of m is uncertain. Since the range of the exponent m is generally known from literature or material handbooks, it is possible to initially assume that the exponent is uniformly distributed between the lower- and upper-bounds. Then, the goal is to narrow the distribution of the exponent using the Bayesian statistics with measured damage sizes.

Since the Paris model is based on crack growth during N cycles, the fundamental idea of this paper is to use the measured crack growth data to characterize the damage parameters. Let the current cycle be N, and the

previous measurement have been performed at $N - \Delta N$. The crack growth between two measurements can be defined as

$$\Delta a_N = a_N - a_{N-\Delta N} \tag{7}$$

If the measured damage sizes are accurate, the crack growth calculation will be accurate. However, due to noise and bias of SHM system, the measured crack growth will have uncertainty. In the following, we will explain how this uncertain crack growth can be used to narrow the distribution of damage parameters.

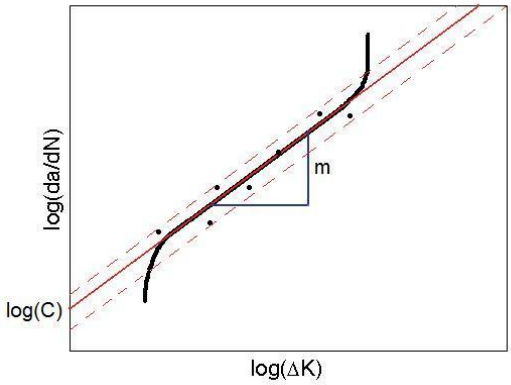

Figure 1. Illustration of Paris law parameter in a log-log plot of crack growth rate.

Bayesian update is based on Bayes' theorem on conditional probability. It is a technique commonly used to obtain the updated (also called posterior) probability of a random variable by using new information available for the variable. In this paper, since the probability distribution is of interest, we used the following form of Bayes' theorem that can fit for our purpose (An, et al. (2008)):

$$f_{updt}(m) = \frac{P(\Delta a|m) f_{ini}(m)}{\int_{-\infty}^{+\infty} P(\Delta a|m) f_{ini}(m) dm} \tag{8}$$

where m is the variable we want to update, f_{ini} the assumed (or prior) probability density function (PDF) of m, f_{updt} the updated (or posterior) PDF of m and $P(\Delta a|m)$ is called the likelihood function, which is the probability of obtaining the measured damage growth, Δa, for a given value of m. The integral in the denominator is required in order to make the area under the updated PDF to be one.

The likelihood function is designed to integrate the information obtained from inspection to the knowledge we have about the distribution of m. In this paper, we choose the damage growth between two consecutive inspections as the measurement outcome, in other words the information we use to update the distribution of m. Thus, it is the probability to have the measured damage growth for a given m. In general, the measured damage growth includes the effect of bias and noise of the sensor measurement. With a large number of measurements, however, it is possible to narrow the distribution of m from its initial wide distribution.

Let a_N be the true crack size, b the bias, and v the noise. The measured crack size, a_N^{meas}, is then given as

$$a_N^{meas} = a_N + b + v \tag{9}$$

The measurement bias b reflects a deterministic bias, such as calibration bias, while the noise v reflects random noise. For subsequent measurements, the bias b remains constant, while the noise v will vary uniformly with maximum range V. That expression can be used to define the damage growth between consecutive inspections as follows

$$\Delta a_N^{meas} = a_N^{meas} - a_{N-\Delta N}^{meas} = \Delta a_N - \Delta v_N \tag{10}$$

At a given inspection, if the measured crack size is assumed to be uniformly distributed due to uniformly distributed noise, then the crack growth is triangularly distributed. Thus, the respective distributions can be found below:

$$\begin{cases} a_N^{meas} \sim U(a_N + b - V\ ;\ a_N + b + V) \\ \Delta a_N^{meas} \sim T(\Delta a_N - 2V; \Delta a_N; \Delta a_N + 2V) \end{cases} \tag{11}$$

The likelihood function is then defined as the probability for a given m to have the measured crack growth. Since the measured data (crack growth) is different from the updated distribution (Paris exponent m), Monte Carlo simulation (MCS) is used to calculate the likelihood function. The likelihood value at the particular m is the value of PDF in Eq. (11) at Δa_N^{meas}. Since this value will change due to bias and noise, the MCS is performed with a sample size M. The MCS involves simulating an initial crack based on the measured crack size, calculate the crack growth using Paris' law and calculate the likelihood as described previously and then those likelihoods are averaged to obtain the value that is used for the likelihood value at a given m. The numerical experiments showed that M = 2,000 is enough to obtain a smooth distribution of the likelihood function. Figure 2 compares the RULs obtained using the true bias with those obtained by ignoring the bias. In all cases, V = 1mm is used. It turns out that the effect of bias on RUL is not significant.

The distribution of RUL is calculated at every inspection using MCS as well but with a larger sample, 50,000 true crack sizes are estimated using the following distribution in Eq. (12) and the RUL is estimated using Eq. (13) derived from Paris' law. This allows us to estimate the distribution and from there obtain the 95% quantile shown in Figure 2.

$$a_N^{true} \sim U(a_N^{meas} - b - V\ ;\ a_N^{meas} - \mathrm{b} + \mathrm{V}) \tag{12}$$

$$N_f = \frac{a_C^{1-\frac{m}{2}} - (a_N^{true})^{1-\frac{m}{2}}}{C\left(1-\frac{m}{2}\right)(\sigma\sqrt{\pi/2})} \tag{13}$$

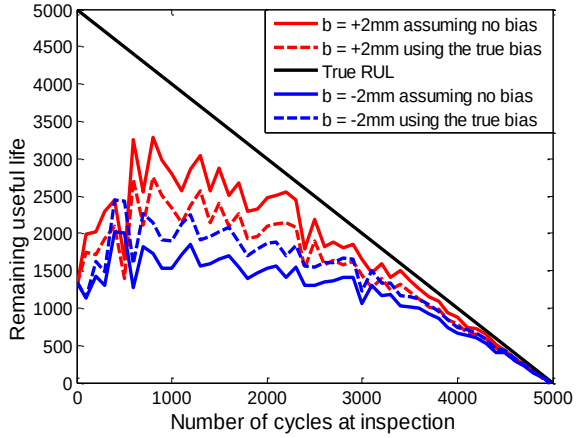

Figure 2. Effect of knowledge of bias in the likelihood on the 95% confidence prediction of RUL

Figure 3 shows the cumulative density function (CDF) of the RUL after 1,000 and 2,000 cycles. The total life of the structure is about 5,000 cycles and it can be observed that the estimated mean RUL is about 5,000 and 3,000 after 1,000 and 2,000 cycles respectively, whereas the 95% confidence estimate it 2,300 and 2,000 cycles. Note that the first two vertical lines show the 5% percentile of each CDF, which corresponds to the 95% confidence RUL prediction. This shows the convergence of RUL as the distribution of m is updated.

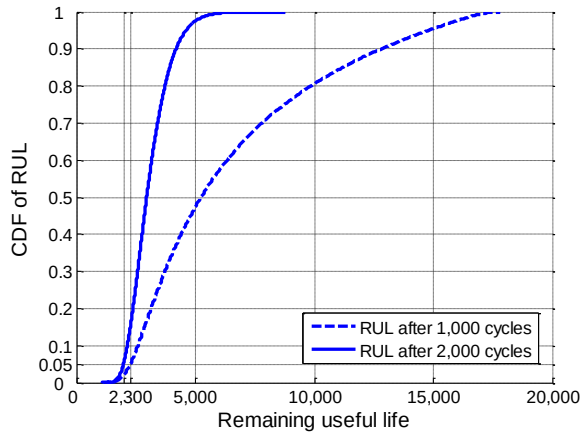

Figure 3. Cumulative density function of RUL for measurements with no bias and minimal noise V = 1mm

One of the major advantages of SHM is that measurements can be performed frequently. Thus, the update in Eq. (8) can be performed as frequently as needed. However, since the damage grows slowly and the bias and noise of measurements are in general large, too frequent measurements may not help to narrow the distribution of damage parameters.

4 NUMERICAL APPLICATION

This paper presents two different kinds of results due to the difference between two sets of measurements resulting from the same true crack growth. The results presented previously as well as the updated distribution results for both m and C are obtained using a single set of measurement. The RUL on the other hand is actually the mean of the 95% confidence RUL over 100 sets of measurements this in order to give an estimate of the validity of our method.

Typical material properties for 7075-T651 aluminum alloy are presented in Table 1. The applied fuselage pressure differential is 0.06 *MPa*, obtained from Niu (1990) and the stress is given by Eq. (3). Paris law parameters m and C are obtained using a crack growth rate plot published by Newman, et al. (1999). Note that due to scatter of the crack growth rate, the exponent m and $\log(C)$ are assumed to be uniformly distributed between the lower- and upper-bounds.

Table 1. Geometry, loading and fracture parameters of 7075-T651 Aluminum alloy

Property	Distribution type
Pressure, p (*MPa*)	Lognormal† (0.06,0.003)
Fracture toughness K_{IC} (MPa$\sqrt{meters}$)	Deterministic 30
Fuselage radius r (meters)	Deterministic 3.25
Paris law exponent, m	Uniform‡ (3.3, 4.3)
Damage parameter, $\log(C)$	Uniform (log(5E-11), log(5E-10))

Depending on manufacturing and assembly processes, the actual damage parameters for individual aircraft can be different. For a specific panel, we assume that there exists a true value of deterministic damage parameters. In the following numerical simulation, the true damage will grow according to the true value of damage parameters. On the other hand, the measured damage size will have bias and noise of the measurements. As a first approach to the problem we consider the distributions of m and C separately, which means that when we consider one variable as being uncertain we consider the other one as being known. We chose a couple to compare the prognosis results of both methods, (m = 3.8 and C = 1.5E-10).

From the preliminary damage growth analysis, it was found that the distribution of pressure p has negligible effect on damage growth because the effect

† Lognormal (mean, standard deviation)
‡ Uniform (lower bound, upper bound)

of randomness is averaged out. Thus, in the following analysis, the applied pressure is assumed to be deterministic, 0.06 MPa, the mean of the distribution obtained from Niu (1990).

In general, the minimum size of detectable damage using SHM is much larger than that of the manual inspection. Although different SHM techniques may have different minimum detectable size, we chose an initial crack size $a_0 = 20\,mm$, which is large enough to be detected by most SHM methods. In addition, this size of damage will provide significant crack growth data between the two consecutive inspections.

5 UPDATING OF MATERIAL PROPERTY *m*

In this section, we present how the distribution of the damage parameters for a fuselage panel can be narrowed using SHM and Bayesian update. In order to test the updating procedure, we assume that the actual value m of a particular panel is deterministic, m_{true}, which governs the crack growth. However, the available information is the lower- and upper-bounds of m. Thus, the initial distribution of m is assumed to be uniform to reflect minimum knowledge.

In the example, we assume that the inspection has been performed at every 100 cycles (i.e., $N = 100$). For the results presented here, inspections have been performed on a single panel that contains a crack size that is initially 20 mm until failure of the given panel. The noise in crack detection is assumed to be between -1mm and 1 mm and the bias to be zero. The inspections are conducted until the crack reaches its critical size, a_C, defined in Eq. (6) that has a value about 93 mm.

Figure 4 shows the updated distributions of m for $m_{true} = 3.8$ and $C = 1.5E\text{-}10$. The initial distribution of m is in red, the dotted blue curves are updated distribution (plotted at every 2,000 cycles) and the solid blue curve is the final updated distribution. This is an illustration of the updating process with no bias and small noise ($b = 0$ and $V = 1$mm). It is clear that as the crack grows, the identified distribution of m becomes narrower.

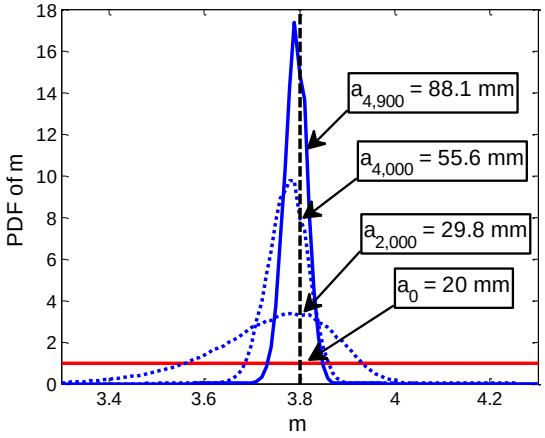

Figure 4. Updated distribution of material parameter *m* for $m_{true} = 3.8$, C = 1.5E-10, (b = 0mm, V = 1mm)

Figure 5 shows the effect of bias on the final updated distribution of m for $m_{true} = 3.8$. The noise is set to the minimum amplitude, 1 mm, in order to emphasize the effect of bias, with for the dotted-dashed line a bias of +2mm and the dotted one a bias of -2mm. It is clear that bias shifts the maximum likelihood point from that of the true value.

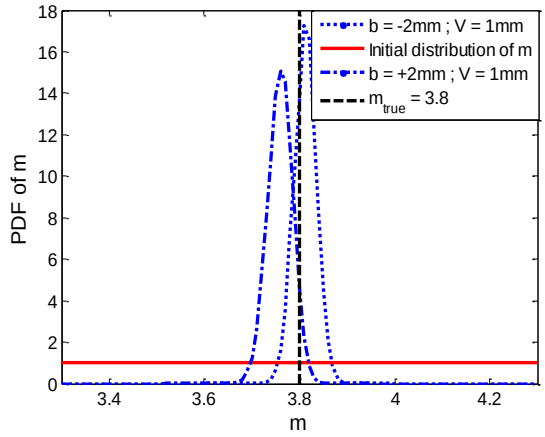

Figure 5. Effect of bias on updated distribution of *m* for $m_{true} = 3.8$, C = 1.5E-10

Figure 6 shows the effect of noise on the distribution of m. The bias is set to the zero in order to emphasize the effect of noise, with for the dotted-dashed line a noise of amplitude 3mm and the dotted one a noise of amplitude 1mm. It is obvious that noise has an effect on the standard deviation but it does not shift the distribution as the bias does.

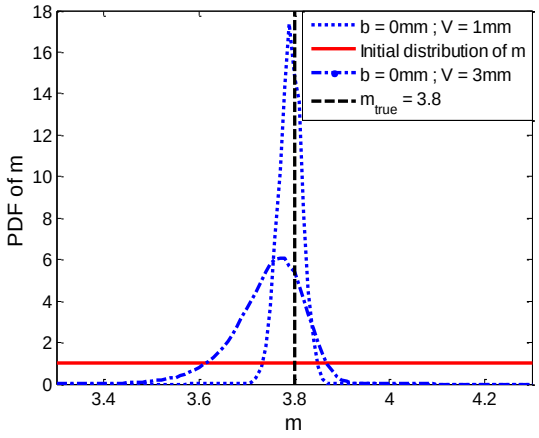

Figure 6. Effect of noise on the updated distribution of m for m_{true} = 3.8, C = 1.5E-10

In addition, Table 2 gives the maximum likelihood, mean and standard deviation of m, corresponding to Figure 5 and Figure 6. It can be observed that the mean and maximum likelihood value are only minimally affected by the bias and noise in the data. However, the standard deviation is large with a large noise. As expected, positive bias (true crack size is smaller than measured) leads to underestimation of m.

Table 2. Statistical characteristics of final distribution for m_{true} = 3.8 and different combinations bias/noise

	Effect of noise		Effect of bias	
Bias, noise (mm)	b = 0 V = 1	b = 0 V = 3	b = -2 V = 1	b = +2 V = 1
Maximum likelihood	3.79	3.78	3.81	3.76
Mean	3.79	3.74	3.81	3.76
Standard deviation	0.02	0.08	0.02	0.03

An important motivation for updating the distribution of m is to improve the accuracy of prognosis for a specific panel. We will discuss the application to the calculation of the remaining useful life (RUL) at every inspection. In order to show the value of our method we compare RUL calculated using the actual value of m, m_{true}, and the 95% quantile of the distribution of RUL obtained using the updated distribution of m at each inspection and 95% confidence RUL obtained using the initial distribution of m, this is shown in Figure 7. The figure shows the true remaining useful life compared to the 95% quantile obtained for two couples bias/noise that correspond to the extreme cases, most and least conservative estimates of RUL and the 95% confidence RUL obtained using the handbook distribution.

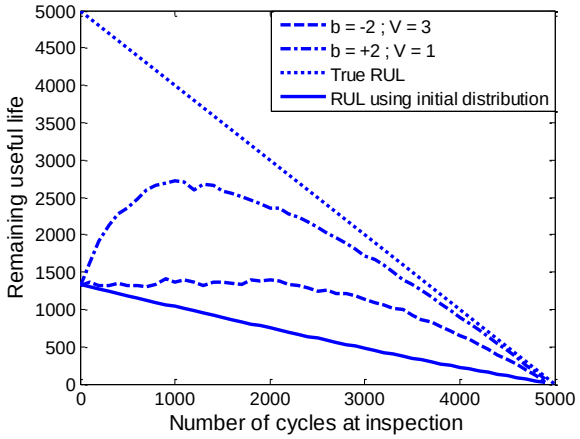

Figure 7. 95% confidence RUL after inspection compared to true RUL

It can be observed that the updated distribution of m allows us to have conservative estimate of the RUL that converges to the actual value. We can also observe that we have a significantly more accurate prognosis then the one obtained using the handbook distribution.

6 UPDATING OF MATERIAL PROPERTY *C*

In this section, the other Paris parameter, C, will be updated instead of m. Since Paris law becomes linear in log-log scale, log(C) will have comparable effect with m. Thus, we choose to actually update the distribution of log(C) to have a distribution of the same order as m. The updating process is the same as described earlier with the same type of likelihood function and the same noise and bias.

In this case we fix m to 3.8, the true value used for updating earlier, and the true value C is chosen to be 1.5E-10, the value it was fixed at in the previous section. Figure 8 shows the updated distributions of C with m_{true} = 3.8. The initial distribution of C is in red, the dotted blue curves are updated distribution (plotted at every 2,000 cycles) and the solid blue curve is the final updated distribution. This is an illustration of the updating process with no bias and small noise (b = 0 and V = 1mm). It is clear that as the crack grows, the identified distribution of C becomes narrower.

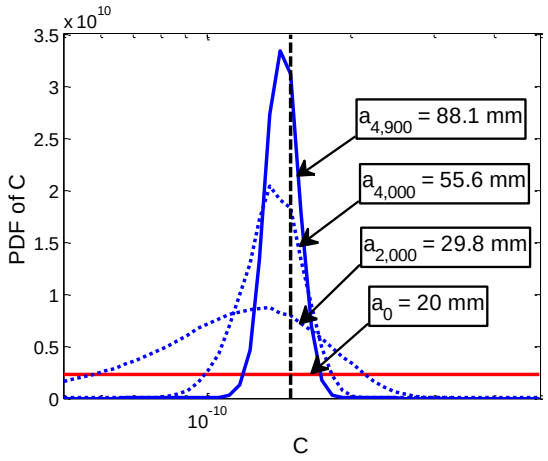

Figure 8. Updated distribution of material parameter *C* for C_{true} = 1.5E-10, *m* = 3.8, (b = 0mm, V = 1mm)

The effects of noise and bias turn out to be similar to the case of updating *m*. Figure 9 shows the effect of bias on the final updated distribution of *C* for C_{true} = 1.5E-10. As for *m*, the noise is set to the minimum amplitude, 1 mm, in order to emphasize the effect of bias, with for the dotted-dashed line a bias of +2mm and the dotted one a bias of -2mm. As for *m*, bias appears to shift the maximum likelihood point from that of the true value.

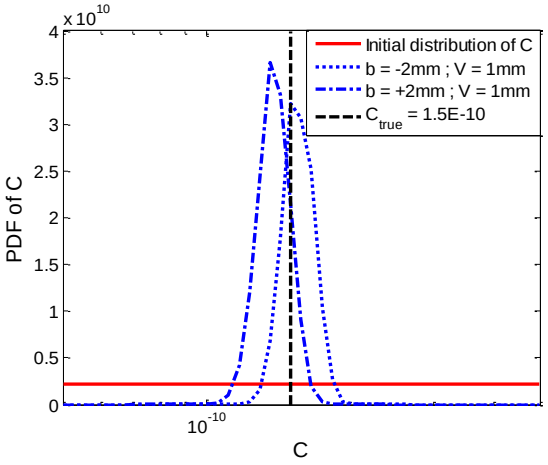

Figure 9. Effect of bias on the updated distribution of *C* for m_{true} = 3.8, C = 1.5E-10

Figure 10 shows the effect of noise on the distribution of *C*. The bias is set to the zero in order to emphasize the effect of noise, with for the dotted-dashed line a noise of amplitude 3mm and the dotted one a noise of amplitude 1mm. It is obvious that noise increases the standard deviation but it does not shift the distribution as the bias does.

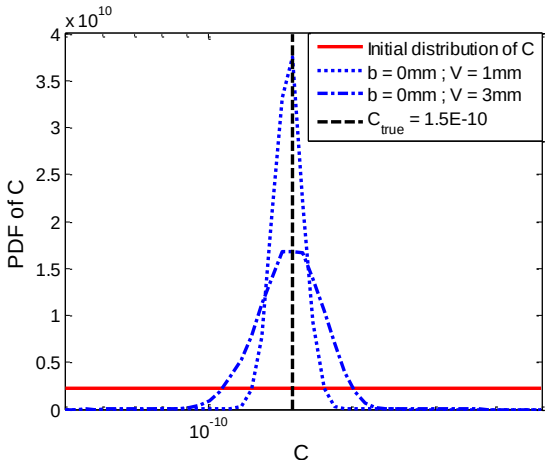

Figure 10. Effect of noise on final distribution of *C* for C_{true} = 1.5E-10, *m* = 3.8

Table 3 gives the maximum likelihood, mean and standard deviation of, *C* corresponding to Figure 9 and Figure 10. It can be observed that the mean is only minimally affected by the bias and noise in the data. However, the standard deviation is large with large noise. As expected, positive bias (true crack size is smaller than measured) leads to underestimation of *m*.

Table 3. Statistical characteristics of updated distribution for C_{true} = 1.5E-10 and different bias/noise

	Effect of noise		Effect of bias	
Bias, noise (mm)	b = 0 V = 1	b = 0 V = 3	b = -2 V = 1	b = +2 V = 1
Maximum likelihood	1.4E-10	1.4E-10	1.8E-10	1.4E-10
Mean	1.5E-10	1.4E-10	1.5E-10	1.4E-10
Standard deviation	1.2E-11	2.4E-11	1.2E-11	1.0E-11

We will now discuss the application of the updated distribution of *C* to the calculation of RUL at every inspection. In order to show the accuracy of the proposed method, we compare RUL calculated using the actual value of *C*, C_{true}, and the 95% quantile of the distribution of RUL obtained using the updated distribution of *C* at each inspection and 95% confidence RUL obtained using the initial distribution of *C*, which is shown in Figure 11. The figure shows the true RUL compared to the 95% quantile obtained for two couples bias/noise that correspond to the extreme cases, most and least conservative estimates of RUL and the 95% confidence RUL obtained using the handbook distribution.

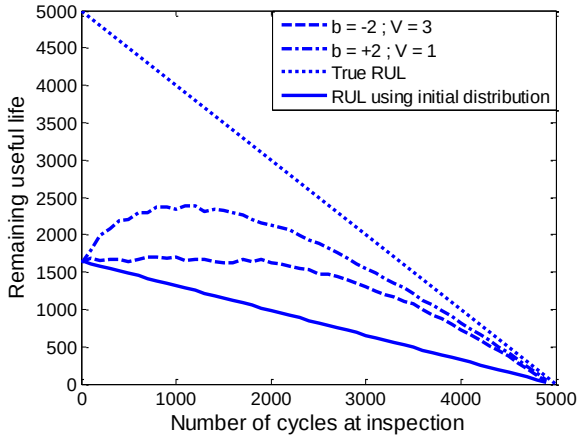

Figure 11. 95% confidence RUL after inspection compared to true RUL

It can be observed that the updated distribution of C allows us to have conservative estimate of the RUL that converges to the actual value. The gain in accuracy with respect to the handbook distribution does not vary much compared to what we obtained using m, the two variables appear to have an equivalent effect.

7 CONCLUSION

In this paper, a Bayesian updating technique is employed to identify panel-specific damage growth parameters using damage sizes measured from SHM sensors. The actual measurement environment is modeled by introducing deterministic bias and random noise.

When there is no bias, the probability distributions of the two Paris parameters, m and C, are effectively narrowed and converged to the true values. The large number of SHM measurements compensates the effect of noise, and thus, the identified damage parameters are relatively insensitive to the noise. However, the effect of bias remains and affects the identification of true material parameters. It is shown that the convergence is slow when the bias is negative and noise is large, while the convergence is fast when the bias is positive and the noise is small. However, the latter yields underestimation of the true parameters.

The identified distributions of parameters are used to estimate the remaining useful life (RUL) with 95% confidence. In all combined cases with noise and bias, the proposed method converges to the true RUL from the conservative side.

ACKNOWLEDGMENT

This work was supported by the Air Force Office of Scientific Research under Grant FA9550-07-1-0018 and by the NASA under Grant NNX08AC334.

NOMENCLATURE

a	crack size
a^{meas}	measured crack size
a_0	initial crack size
a_C	critical crack size
a_N	crack size at Nth inspection
a_{true}	true crack size
b	bias in damage size measurement
C	Paris law parameter
f_{ini}	initial (or prior) probability density function (PDF)
$f_{i,test}$	likelihood function
f_{updt}	updated (or posterior) PDF
K_{IC}	fracture toughness
m	Paris law exponent
M	Monte-Carlo simulation sample size
N	step between inspections
p	pressure
r	fuselage radius
t	panel thickness
v	noise in damage size measurement
V	range of noise in damage size measurement
Δa	crack growth
Δa^{meas}	measured crack growth
ΔK	range of stress intensity factor
σ	applied stress

REFERENCES

J. An, E. Acar, R. T. Haftka, N. H. Kim, P. G. Ifju, and T. F. Johnson. (2008). Being Conservative with a Limited Number of Test Results, *Journal OF Aircraft*, vol. 45, pp. 1969-1975.

P. Berruet, A. K. A. Toguyeni, and E. Craye. (1999, Structural and functional approach for dependability in FMS, in *IEEE International Conference on Systems, Man, and Cybernetics*

S. J. Engel, B. J. Gilmartin, K. Bongort, and A. Hess. (2000, March 18-25), Prognostics, the real issues involved with predicting liferemaining, in *IEEE Aerospace Conference*, Big Sky, MT

K. Goebel, B. Saha, A. Saxena, N. Mct, and N. Riacs. (2008). A comparison of three data-driven techniques for prognostics,

J. Gu, D. Barker, and M. Pecht. (2007), "Uncertainty Assessment of Prognostics of Electronics Subject to Random Vibration," in *AAAI Fall Symposium on Artificial Intelligence for Prognostics*, pp. 50-57.

H. H. Harkness. (1994). *Computational methods for fracture mechanics and probabilistic fatigue*. Ph.D. thesis, the Northwestern University, Evanston, IL

L. C. Jaw, S. M. Inc, and A. Z. Tempe. (1999, Neural networks for model-based prognostics, in *IEEE Aerospace Conference*

A. A. Kale, R. T. Haftka, M. Papila, and B. V. Sankar. (2003), "Tradeoff for Weight and Inspection Cost

for Fail-Safe Design," in *44th AIAA/ASME/SDM conference* Norfolk, VA.

A. A. Kale, R. T. Haftka, and B. V. Sankar. (2004, Tradeoff of structural weight and inspection cost in reliability based optimization using multiple inspection types, in *10th AIAA/ ISSMO Multidisciplinary analysis and optimization conference*, Albany, NY

A. A. Kale, R. T. Haftka, and B. V. Sankar. (2008). Efficient Reliability-Based Design and Inspection of Stiffened Panels Against Fatigue, *Journal OF Aircraft*, vol. 45, p. 86.

C. J. Li and H. Lee. (2005). Gear fatigue crack prognosis using embedded model, gear dynamic model and fracture mechanics, *Mechanical systems and signal processing*, vol. 19, pp. 836-846.

K. Y. Lin, D. T. Rusk, and J. J. Du. (2002). Equivalent level of safety approach to damage-tolerant aircraft structural design, *Journal of Aircraft*, vol. 39, pp. 167-174.

J. Luo, M. Namburu, K. Pattipati, L. Qiao, M. Kawamoto, and S. Chigusa. (2003, Model-based prognostic techniques [maintenance applications], in *IEEE Systems Readiness Technology Conference*

G. C. Montanari. (1995). Aging and life models for insulation systems based on PD detection, *IEEE Transactions on Dielectrics and Electrical Insulation*, vol. 2, pp. 667-675.

J. C. Newman, E. P. Phillips, and M. H. Swain. (1999). Fatigue-life prediction methodology using small-crack theory, *International Journal of fatigue*, vol. 21, pp. 109-119.

M. Niu. (1990), "Airframe Structural Design," in *Fatigue, Damage Tolerance and Fail-Safe Design*, Conmilit Press LTD., Ed. Hong Kong, pp. 538-570.

M. Orchard, G. Kacprzynski, K. Goebel, B. Saha, and G. Vachtsevanos. (2008, Advances in Uncertainty Representation and Management for Particle Filtering Applied to Prognostics, in *International Conference on Prognostics and Health Management,*, Denver, CO

M. Orchard, B. Wu, and G. Vachtsevanos. (2005, A Particle Filter Framework for Failure Prognosis, in *World Tribology Congress III*, Washington, D.C.

P. C. Paris, H. Tada, and J. K. Donald. (1999). Service load fatigue damage—a historical perspective, *International Journal of fatigue*, vol. 21, pp. 35-46.

A. Ray and R. Patankar. (1999). A stochastic model of fatigue crack propagation under variable-amplitude loading, *Engineering Fracture Mechanics*, vol. 62, pp. 477-493.

A. Ray and S. Tangirala. (1996). Stochastic modeling of fatigue crack dynamics for on-line failure prognostics, *IEEE Transactions on Control Systems Technology*, vol. 4, pp. 443-451.

B. Saha and K. Goebel. (2008, Uncertainty Management for Diagnostics and Prognostics of Batteries using Bayesian Techniques, in *IEEE Aerospace Conference*

M. A. Schwabacher. (2005, A survey of data-driven prognostics, in *AIAA Infotech@Aerospace Conference*, Reston, VA

J. W. Sheppard, M. A. Kaufman, A. Inc, and M. D. Annapolis. (2005). Bayesian diagnosis and prognosis using instrument uncertainty, *IEEE Autotestcon, 2005*, pp. 417-423.

A. N. Srivastava and S. Das. (2009). Detection and Prognostics on Low Dimensional Systems, *IEEE Transactions on Systems, Man, and Cybernetics, Part C: Applications and Reviews*, vol. 39, pp. 44-54.

M. Tipping. (2000), "The Relevance Vector Machine. in Advances in Neural Information Processing Systems," MIT Press, Cambridge.

L. Wang and F. G. Yuan. (2005). Damage identification in a composite plate using prestack reverse-time migration technique, *Structural Health Monitoring*, vol. 4, pp. 195-211.

Y. Xue, D. L. McDowell, M. F. Horstemeyer, M. H. Dale, and J. B. Jordon. (2007). Microstructure-based multistage fatigue modeling of aluminum alloy 7075-T651, *Engineering Fracture Mechanics*, vol. 74, pp. 2810-2823.

J. Yan and J. Lee. (2007, A Hybrid Method for On-line Performance Assessment and Life Prediction in Drilling Operations, in *IEEE International Conference on Automation and Logistics*